

ORIGINAL
RESEARCH

A. Rossi
R. Biancheri
F. Zara
C. Bruno
G. Uziel
M.S. van der Knaap
C. Minetti
P. Tortori-Donati



Hypomyelination and Congenital Cataract: Neuroimaging Features of a Novel Inherited White Matter Disorder

BACKGROUND AND PURPOSE: Hypomyelination and congenital cataract (HCC) is an autosomal recessive white matter disease caused by deficiency of hyccin, a membrane protein implicated in both central and peripheral myelination. We aimed to describe the neuroimaging features of this novel entity.

MATERIALS AND METHODS: A systematic analysis of patients with unclassified leukoencephalopathies admitted to our institutions revealed 10 children with congenital cataract, slowly progressive neurologic impairment, and diffuse white matter abnormalities on neuroimaging. Psychomotor developmental delay was evident after the first year of life. Peripheral neuropathy was demonstrated by neurophysiologic studies in 9 children. The available neuroimaging studies were retrospectively reviewed.

RESULTS: In all patients, neuroimaging revealed diffuse involvement of the supratentorial white matter associated with preservation of both cortical and deep gray matter structures. Supratentorial white matter hypomyelination was detected in all patients; 7 patients also had evidence of variably extensive areas of increased white matter water content. Deep cerebellar white matter hypomyelination was found in 6 patients. Older patients had evidence of white matter bulk loss and gliosis. Proton MR spectroscopy showed variable findings, depending on the stage of the disease. Sural nerve biopsy revealed hypomyelinated nerve fibers. Mutations in the *DRCTNNB1A* gene on chromosome 7p15.3, causing complete or severe deficiency of hyccin, were demonstrated in all patients.

CONCLUSIONS: HCC is characterized by a combined pattern of primary myelin deficiency and secondary neurodegenerative changes. In the proper clinical setting, recognition of suggestive neuroimaging findings should prompt appropriate genetic investigations.

Leukoencephalopathies constitute a large heterogeneous group of disorders whose underlying metabolic abnormality often remains obscure, despite extensive investigations. Studies have shown that a specific diagnosis remains undetermined in as many as 50% of children with a leukoencephalopathy.¹ However, genetic research has greatly contributed to the understanding of the etiologic background of several white matter disorders in the last decade, providing new insight into the disease inheritance pattern and risk of familial recurrence as well as offering a method for prenatal diagnosis.²

The term hypomyelination indicates reduced or absent myelin deposition that may involve the central nervous system, the peripheral nervous system, or both. Several hypomyelinating disorders are known, including Pelizaeus-Merzbacher disease, Salla disease, Cockayne syndrome type II, Tay syndrome, and hypomyelination with atrophy of the basal ganglia and cerebellum.³ However, hypomyelinating disorders still represent the largest single category among unclassified leukoencephalopathies.¹

Hypomyelination and congenital cataract (HCC) (Online Mendelian Inheritance in Man, No. 610532) is a recently de-

scribed autosomal recessive white matter disorder characterized by central and peripheral hypomyelination, slowly progressive neurologic impairment, and congenital cataract, caused by a deficiency of a novel membrane protein, hyccin, encoded by the *DRCTNNB1A* gene located on chromosome 7p15.3.⁴ We aimed to describe the neuroimaging findings in 10 patients affected by this novel disease entity.

Methods

A systematic analysis of patients with unclassified leukoencephalopathies admitted to our institutions revealed 10 children (8 boys and 2 girls) from 5 unrelated families (4 of Italian origin and 1 from Turkey) presenting with congenital cataract, slowly progressive neurologic impairment, and diffuse white matter abnormalities on MR imaging. Three families were consanguineous. All patients were born at term and had normal prenatal and perinatal histories. Their head circumferences were normal. All patients had bilateral cataracts at birth or within the first month of life and underwent ocular surgery within 6 months of birth. Retrospective analysis of ophthalmologic data indicated that the congenital cataract was total in 6 patients. Early developmental milestones were normal in all patients. Developmental delay was detected after the first year of life, and 3 patients experienced a few seizures. All patients achieved the ability to walk with support between 12 months and 2 years of age. Unsupported walking was not achieved in any patient. The patients showed no severe clinical worsening, but most of them gradually lost their ability to walk, becoming wheelchair-bound. The age of last observation ranged from 2 to 27 years.

On neurologic examination, all patients had dysarthria, truncal hypotonia, brisk tendon reflexes, and bilateral extensor plantar responses. Peripheral neuropathy was revealed by muscle weakness and

Received March 15, 2007; accepted after revision July 10.

From the Department of Pediatric Neuroradiology (A.R., P.T.-D.) and Muscular and Neurodegenerative Diseases Unit (R.B., F.Z., C.B., C.M.), G. Gaslini Children's Research Hospital, Genoa, Italy; Department of Child Neurology (G.U.), C. Besta National Neurological Institute, Milan, Italy; and Department of Child Neurology (M.S.v.d.K.), VU University Medical Center, Amsterdam, the Netherlands.

Please address correspondence to Andrea Rossi, MD, Department of Pediatric Neuroradiology, G. Gaslini Children's Research Hospital, Largo G. Gaslini 5, 16147 Genoa, Italy; e-mail andrea.rossi@ospedale-gaslini.ge.it

indicates article with supplemental on-line table

DOI 10.3174/ajnr.A0792

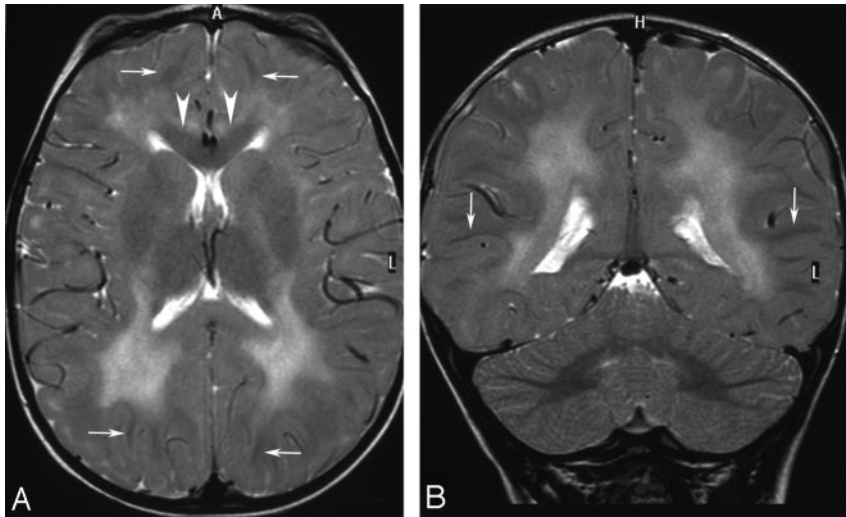


Fig 1. HCC: early stage (patient 8, 20 months of age). Axial (A) and coronal (B) T2-weighted images (4157/100/2, TR/TE/NEX) show diffuse hyperintensity of the deep, periventricular, and capsular white matter with local sparing of the subcortical white matter (arrows, A and B) and callosal genu (arrowheads, A). The cerebellum is fully myelinated (B).

wasting in the lower limbs and was confirmed by motor nerve conduction velocity (NCV) findings in 9 patients. The NCV studies were performed at the same time as the first neuroimaging studies and were re-evaluated, in some cases, during the follow-up. Sural nerve biopsy was performed in 4 patients after initial neuroimaging studies, and it showed lack of myelin with slight-to-severe reduction of myelinated fiber attenuation, sometimes with evidence of small onion bulbs formed by Schwann cell processes wrapping around thinly myelinated axons. In all patients, genetic studies revealed mutations of the *DRCTNNB1A* gene on chromosome 7p15.3, causing complete or severe deficiency of hyccin, a novel 521 amino acid protein.

MR imaging was performed in 9 patients. Two patients underwent 2 examinations each, 1 patient underwent 3 examinations, and 1 patient underwent only CT. Patient age ranged between 20 months and 26 years at the time of the initial study. Because the imaging studies were performed at various times and institutions, MR image parameters, static magnetic field power (0.5, 1, and 1.5T), and gradient field strength of the MR imaging scanners varied among the indi-

vidual patients. However, axial and/or sagittal T1-weighted spin-echo (400–650/12–20/1–3, TR/TE/NEX) and axial T2-weighted fast spin-echo images (2300–5782/90–150/1–6, TR/TE/NEX) were always available for review. Axial and/or coronal fluid-attenuated inversion recovery (FLAIR) images (6000–15,000/109–150/1–2, TR/TE/NEX; 1800–2200, TI) were obtained in 11 out of 13 available MR imaging examinations. Postcontrast T1-weighted spin-echo images were obtained in 2 patients. Diffusion-weighted echo-planar imaging (DWI) (3449/67/1, TR/TE/NEX; $b = 0$ and 1,000) and localized proton MR spectroscopy were performed in 5 patients (patients 2, 7, 8, 9, and 10). In 4 of them (patients 2, 7, 8, and 9), MR spectroscopy was performed with a point-resolved spectroscopy technique (PRESS) (TR, 2,000; NEX, 128). An $18 \times 18 \times 18$ mm region of interest was manually placed on the abnormal white matter of the left parietal lobe so as to avoid or minimize contamination by CSF and gray matter, and 2 different sequences were performed at short (ie, 23 ms) and intermediate (ie, 144 ms) TEs. The resulting spectra were analyzed qualitatively by visual inspection and computerized numeric analysis, resulting in determinations of ratios of the principal metabolites. These spectra were compared with identically processed spectra of normal age-matched individuals developed at one of our institutions. In 1 patient (patient 10), MR spectroscopy was performed by using a short echo time stimulated echo acquisition mode (STEAM) sequence (6000/10/64, TR/TE/NEX). Single-acquisition reference measurements without water suppression were acquired additionally to enable eddy-current correction. The spectra were ac-

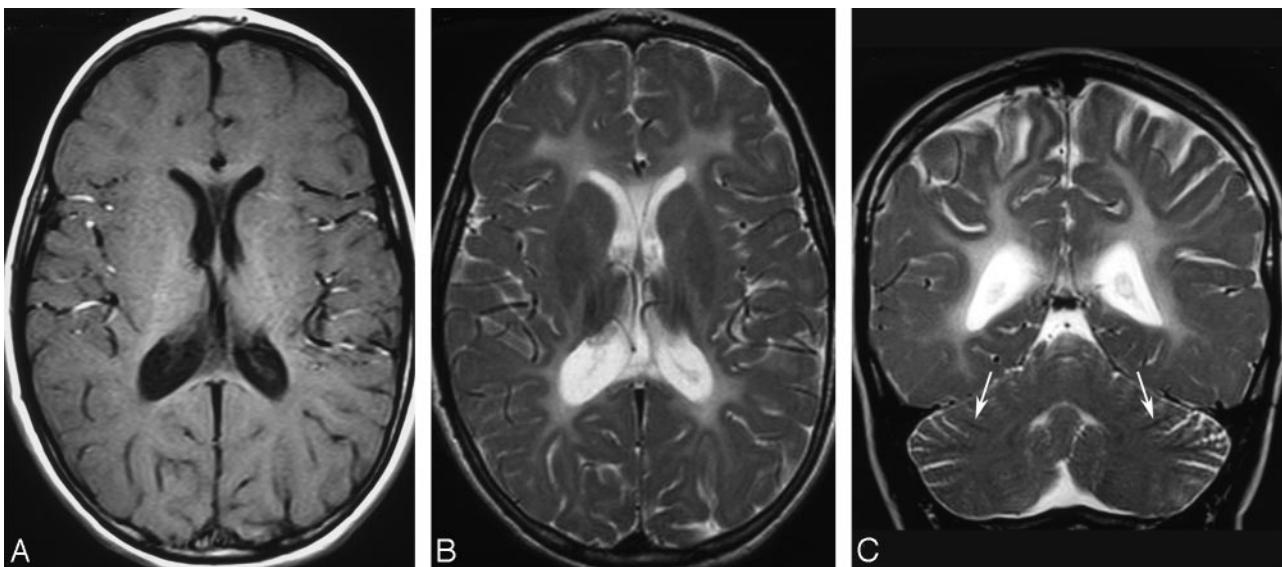


Fig 2. HCC: intermediate stage (patient 6, 8 years of age). A, Axial T1-weighted image (513/12/2, TR/TE/NEX) shows diffuse mild hypointensity of the supratentorial white matter, resulting in blurred gray-white matter interface, consistent with hypomyelination. B, Axial T2-weighted image (4500/108/4, TR/TE/NEX) shows moderate diffuse white matter hyperintensity, also consistent with hypomyelination. Note that the signal intensity is significantly lower than that of CSF. C, Coronal T2-weighted image (4531/112/4, TR/TE/NEX) shows mild hyperintensity of the white cores of the cerebellar hemispheres as well as residual myelination of the medullary laminae (arrows).

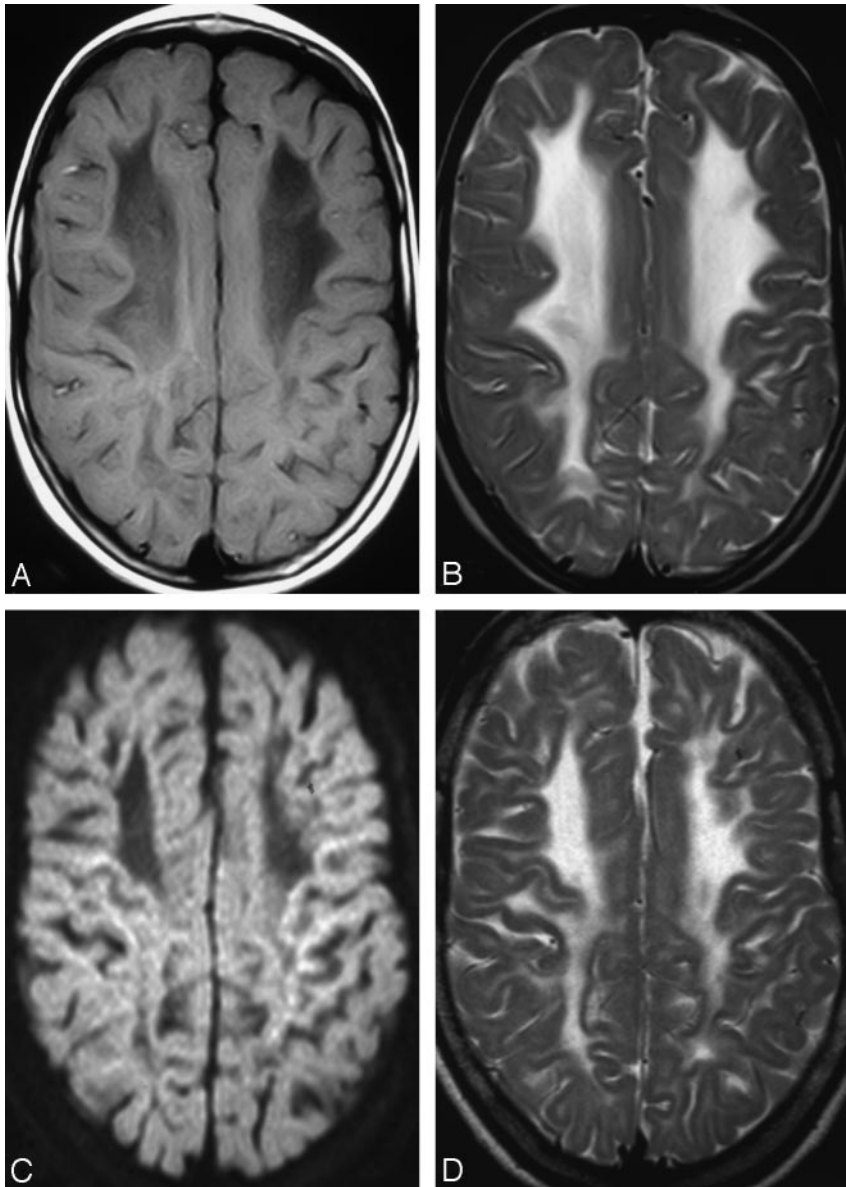


Fig 3. HCC: intermediate and chronic stages (patient 7). *A*, Axial T1-weighted image (437/16/2, TR/TE/NEX) obtained at 8 years of age shows hypointense deep and periventricular white matter, with an anterior-to-posterior gradient of severity. *B*, Axial T2-weighted image (4000/96/2, TR/TE/NEX) obtained at 8 years of age shows marked white matter hyperintensity, paralleling that of CSF and prevailing in the frontal regions. *C*, Axial DWI obtained at 15 years of age shows shrunken white matter with markedly increased diffusivity. The ADC value in deep frontal white matter was 2.094 mm²/s. *D*, Axial T2-weighted image (4157/100/2, TR/TE/NEX) confirms shrinkage of affected white matter (compare with *B*).

aging studies consistently revealed diffusely elevated T2 signal intensity of the supratentorial white matter, associated with preservation of both cortical and deep gray matter structures. All supratentorial white matter regions displayed abnormal signal intensity in all patients except 2 (patients 8 and 9) in whom the subcortical white matter was partially spared (Fig 1). The degree of T2 hyperintensity was intermediate between that of myelinated white matter and CSF, whereas T1-weighted images showed an isointense to slightly hypointense signal intensity, consistent with diffuse hypomyelination (Fig 2). Furthermore, in 7 patients, there was additional evidence of an associated abnormality consisting of areas of higher T2 signal intensity, with corresponding low signal intensity in T1-weighted images, consistent with areas of increased white matter water content. The size of these areas was variable, ranging from small areas in the deep frontal white matter to marked periventricular abnormalities with larger extension in the frontal lobes and less extensive involvement of the peritrigonal areas (Fig 3). In 2 of these patients, marked hypointensity on FLAIR images suggested liquefaction. On follow-up studies, shrinkage of the affected white matter was seen in the same regions (Fig 3). There was a gross correlation between white matter volume and patient age, in that younger patients (patients 1, 2, 4, 7, 8, and 9) had a greater amount of white matter than older ones (patients 3, 5, and 10), who by contrast had an atrophic gliotic white matter with associated enlargement of the ventricular system and subarachnoid spaces. Abnormal contrast enhancement was not detected in the patients receiving gadolinium chelate intravenously.

The corpus callosum was normal in 2 patients (patients 8 and 9, the youngest in this series) and thinned in the remainder. The cerebellum was normal in size in all patients, and myelination of the medullary laminae was consistently normal. Conversely, in 6 patients, the medullary centers of the cerebellar hemispheres showed mildly increased T2 signal intensity, paralleling that of the adjacent cortical gray matter and resulting in a “blurred” gray-white matter interface (Fig 1). The brain stem was normal in 2 patients (patients 1 and 9); in another 2 patients, the brain stem was normal in size but contained signal-intensity abnormalities,

quired from a volume of interest (VOI) of the parietal white matter (6 mL) and the mid parieto-occipital cortex (6 mL). Metabolite concentrations were calculated by using the LCModel⁵ and expressed as mmol/L VOI.

The neuroimaging studies were reviewed in consensus by 2 expert neuroradiologists (A.R., P.T.-D.), who were blinded to the clinical history and neurologic findings. Regarding image analysis, the cerebral white matter was divided into subcortical white matter (arcuate [or U] fibers), periventricular white matter (a rim of white matter abutting the ventricular lining), and deep white matter (the zone between arcuate fibers and periventricular white matter); and the signal intensity in all available sequences was recorded. White matter signal-intensity abnormalities were also sought in the cerebellum and brain stem. Where available, follow-up MR imaging studies were compared with the initial images to evaluate deterioration or static disease.

Results

A summary of clinical and neuroradiologic findings in this series is provided in the supplemental on-line Table. MR im-

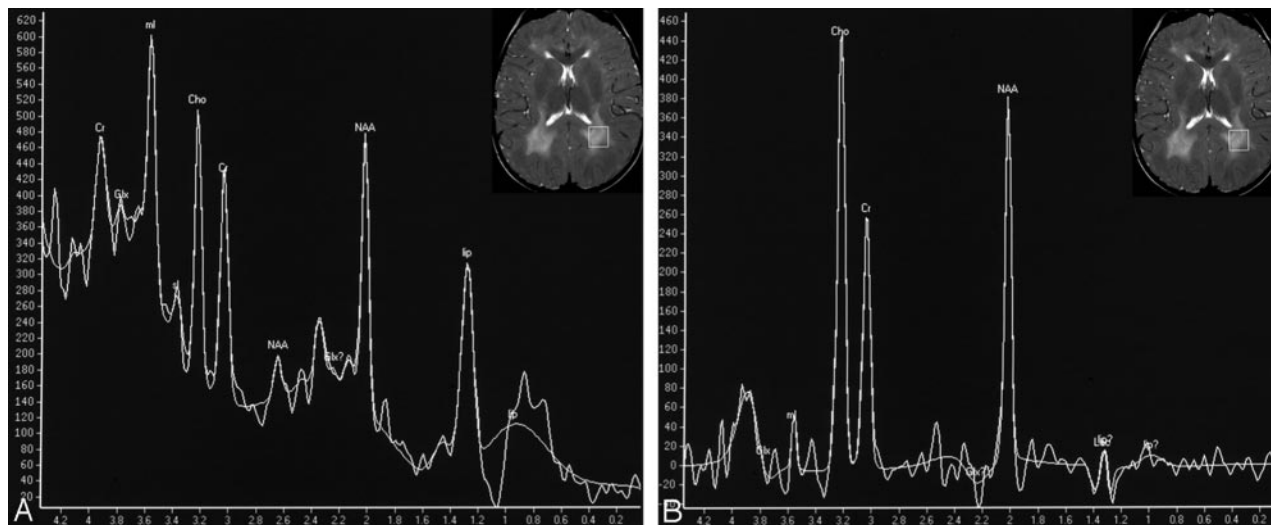


Fig 4. MR spectroscopy findings (patient 8, 20 months of age). On the upper right image corners, axial T2-weighted images (4157/100/2, TR/TE/NEX) show localization of an $18 \times 18 \times 18$ mm region of interest over the right posterior periventricular white matter. **A**, Short echo-time MR spectrum (PRESS; 2000/23 ms, TR/TE) shows elevation of mIns/Cr and Cho/Cr ratios, normal NAA/Cr ratio, and abnormally elevated lipid peak at 1.29 ppm. **B**, Intermediate echo-time MR spectrum (PRESS; 2000/144 ms, TR/TE) confirms elevated Cho/Cr and normal NAA/Cr.

involving the corticospinal tracts (patient 2) and the substantia nigra (patient 8). All the other patients had a moderately hypoplastic pons, associated with hyperintense corticospinal tracts in patient 6 and hyperintense transverse pontine fibers in patient 3. Regarding imaging of the orbits, all patients had already undergone surgery at the time of their neuroimaging studies; as a consequence, changes due to the congenital cataracts could not be evaluated.

Findings on DWI were available for review in 4 patients (patients 2, 7, 8, and 9). The affected white matter showed variably increased diffusivity in all patients. Apparent diffusion coefficient (ADC) values ranged between 1.147 and 1.298 mm^2/s in the hypomyelinated regions and between 1.395 and 2.094 mm^2/s in the areas of increased water content (Fig 3). Areas of restricted diffusion were not detected.

MR spectroscopy gave heterogeneous results, probably due to the different stages of the disease at the time of the various studies (Table). In 2 patients studied during the early stage of the disease (ie, 20 months; patients 8 and 9), the MR spectra showed elevated myo-inositol (mIns)/creatine (Cr) and choline (Cho)/Cr ratios with normal *N*-acetylaspartate (NAA)/Cr; in one of them, there was additional evidence of a prominent lipid peak, in the absence of heterogeneous lipid contamination (Fig 4). Two patients studied in the second decade of life (patients 2 and 7) showed a moderate decrease in the Cho/Cr ratio as the only significant abnormality. In 1 patient studied at 17 years of age (patient 10), quantitative assay of metabolite concentration revealed elevated Cr and mIns, and reduced NAA in the involved white matter.

Discussion

HCC is a recently described inherited white matter disease caused by deficiency of a novel cell membrane protein, hyccin, encoded by the *DRCTNNB1A* gene on chromosome 7p15.3.⁴ Hyccin appears to play an important, albeit as yet undetermined, role in the process of myelination of both central and peripheral nervous systems, as indicated by evidence of hypomyelination on both brain MR imaging and nerve biopsy findings in this series. MR

imaging findings of HCC included diffuse hypomyelination of the supratentorial white matter, in some cases associated with variably extensive areas of increased water content, eventually leading to white matter gliosis and bulk loss. This suggests a primary developmental myelination disorder associated with a neurodegenerative disorder. More interesting, these findings appear to correlate with the results of neuropathologic studies of the sural nerves, which showed lack of myelin with reduced residual myelin compaction, leading to an increased water content in the affected myelin sheaths.

White matter hypomyelination can be easily recognized on MR imaging because of the combination of high T2 signal intensity, albeit not as high as that of CSF, and the less conspicuous T1 signal-intensity abnormality; the T1-weighted images show isointensity or mild hypointensity of the white matter relative to gray matter, resulting in a blurred gray-white matter interface. MR imaging evidence of hypomyelination is common in children, though its cause often remains undetermined.¹ Hypomyelination may be related to either primary disturbance of myelin formation or to neuronal, oligodendrocytic, or astrocytic dysfunction leading to secondary failure of myelination.⁶ The former mechanism underlies Pelizaeus-Merzbacher disease, which is caused by a defect of the proteolipid protein, a major constituent of the myelin proteolipidic structure; on the other hand, the latter phenomena determine early-onset lysosomal storage disorders, Salla disease, Cockayne syndrome, and trichothiodystrophy.¹ In this series, hypomyelination was widespread in the supratentorial brain, with the sole exception of partial subcortical sparing in 2 patients; conversely, the cerebellum was less markedly involved, with completely normal findings in 3 patients and subcortical white matter preservation in all patients.

Evidence of increased water content in the supratentorial white matter, as shown by areas of higher T2 signal intensity, paralleling that of CSF, was a prominent finding in most patients in the present series. Such a finding was variably severe and independent of the severity or progression of the associated clinical picture. These areas were always symmetric and typically displayed an anterior-to-posterior gradient of severity, with a ten-

endency to extend to the subcortical white matter in the anterosuperior frontal regions. The significance of this MR imaging finding remains unclear in the absence of direct histologic verification. Increased white matter water content occurs in several metabolic diseases, most notably Alexander disease, Canavan disease, megalencephalic leukoencephalopathy with subcortical cysts, and vanishing white matter disease,⁷⁻¹⁰ though the white matter is typically more extensively swollen in these disorders than in HCC, often resulting in global enlargement of the affected hemispheres. In these diseases, white matter edema basically results from a variable combination of abnormal myelin formation and vacuolization. On the basis of imaging findings, one could speculate that similar histopathologic abnormalities could also occur in HCC, though perhaps to a lesser degree. Available follow-up studies, as well as neuroimaging investigations performed in older HCC patients, indicate that shrinkage of the affected white matter, with corresponding water content reduction and gliotic changes, occurs as the disease evolves toward a “burnt-out” stage.

MR spectroscopy is a noninvasive method to obtain information about the metabolic status of tissues. The contribution of MR spectroscopy in the diagnostic work-up of hypomyelinating leukoencephalopathies has been elucidated only in few disorders, most notably Pelizaeus-Merzbacher disease and Salla disease. In the former, MR spectroscopy has shown increased concentrations of NAA, glutamine, mIns, and Cr, as well as reduced Cho concentrations, consistent with enhanced neuroaxonal attenuation, astrogliosis, and reduction of oligodendroglia.¹¹ In Salla disease, elevation of *N*-acetyl resonances results from lysosomal accumulation of *N*-acetylneuraminic acid.¹² The role of MR spectroscopy in the diagnostic work-up of patients with HCC remains to be fully appreciated. There is evidence, however, that the MR spectroscopy pattern grossly correlates with the stage of the disease, in that young patients showed features of ongoing myelin breakdown with elevated mIns/Cr and Cho/Cr as well as increased lipid resonances, which are known to occur during active demyelination phases,¹³ whereas older patients showed alterations that may reflect a condition of neuroaxonal damage and gliosis consistent with the burnt-out stage of the disease.

An important limitation of the present study is that this is a retrospective review of patients studied at different points in time during their disease course. The reported neuroimaging features are, therefore, heterogeneous and include both early and chronic findings. However, available data suggest at least a gross correlation between the natural progression of the disease and the neuroimaging findings. In the early stage (before 2 years of age), abnormal myelination occurs in the capsular, periventricular, and deep white matter with essential sparing of the subcortical regions (Fig 1). This finding, together with MR spectroscopy and neuropathologic data, may support the contention that little myelin is laid down and that most of it will be broken down (ie, a combination of hypomyelination and demyelination is likely to occur early during the course of the disease). In the intermediate stage (approximately 2–10 years), the white matter is diffusely abnormal with a background of diffuse hypomyelination (Fig 2), in most patients associated with periventricular and deep white matter liquefaction, as shown by both conventional MR imaging and DWI findings (Fig 3). In the chronic stage (second to third decades), the disease progresses toward a burnt-out stage with

gliosis and white matter bulk loss (Fig 3). Further studies are required to establish whether the disease can be classified into different stages.

Conclusion

This is the first detailed description of neuroimaging findings in HCC, a novel autosomal recessive white matter disease characterized by central and peripheral myelin involvement associated with congenital cataract.³ Both MR imaging and neuropathologic findings suggest that a combination of primary myelin deficiency and secondary neurodegenerative changes probably occurs during the course of the disease. Neuroimaging findings in these patients appear to be variable. However, evidence of combined hypomyelination and increased periventricular white matter water content in patients with congenital cataracts is a peculiarity of HCC as opposed to other forms of leukodystrophy. Recognition of these findings may prove helpful to prompt further genetic investigations, which are necessary to ultimately establish the diagnosis. Further studies are awaited to shed light on the incidence of HCC among unknown white matter disorders, particularly the hypomyelinating forms, and to reveal possible genotype-phenotype correlations.

Acknowledgments

We thank Zoltán Patay, MD, PhD, Chief of the Section of Neuroradiology at the St. Jude Children’s Research Hospital in Memphis, Tenn, for his help with the interpretation of MR spectroscopy findings and Dr. Anna Capurro from the Scientific Direction of the G. Gaslini Children’s Research Hospital in Genoa, Italy, for assistance in the preparation of this manuscript.

References

1. van der Knaap MS, Breiter SN, Naidu S, et al. **Defining and categorizing leukoencephalopathies of unknown origin: MR imaging approach.** *Radiology* 1999;213:121–33
2. Schiffmann R, van der Knaap MS. **The latest on leukodystrophies.** *Curr Opin Neurol* 2004;17:187–92
3. Zara F, Biancheri R, Bruno C, et al. **Deficiency of hyccin, a newly identified membrane protein, causes hypomyelination and congenital cataract.** *Nat Genet* 2006;38:1111–13. Epub 2006 Sep 3
4. van der Knaap MS, Naidu S, Pouwels PJ, et al. **New syndrome characterized by hypomyelination with atrophy of the basal ganglia and cerebellum.** *AJNR Am J Neuroradiol* 2002;23:1466–74
5. Provencher SW. **Estimation of metabolite concentrations from localized in vivo proton MR spectra.** *Magn Reson Med* 1993;30:672–79
6. Di Rocco M, Rossi A, Parenti G, et al. **Different molecular mechanisms leading to white matter hypomyelination in infantile onset lysosomal disorders.** *Neuropediatrics* 2005;36:265–69
7. van der Knaap MS, Naidu S, Breiter SN, et al. **Alexander disease: diagnosis with MR imaging.** *AJNR Am J Neuroradiol* 2001;22:541–52
8. Brismar J, Brismar G, Gascon G, et al. **Canavan disease: CT and MR imaging of the brain.** *AJNR Am J Neuroradiol* 1990;11:805–10
9. van der Knaap MS, Barth PG, Stroink H, et al. **Leukoencephalopathy with swelling and a discrepantly mild clinical course in eight children.** *Ann Neurol* 1995;37:324–34
10. van der Knaap MS, Barth PG, Gabreels FJ, et al. **A new leukoencephalopathy with vanishing white matter.** *Neurology* 1997;48:845–55
11. Hanefeld FA, Brockmann K, Pouwels PJ, et al. **Quantitative proton MRS of Pelizaeus-Merzbacher disease: evidence of dys- and hypomyelination.** *Neurology* 2005;65:701–06
12. Varho T, Komu M, Sonninen P, et al. **A new metabolite contributing to N-acetyl signal in 1H MRS of the brain in Salla disease.** *Neurology* 1999;52:1668–72
13. Degaonkar MN, Khubchandani M, Dhawan JK, et al. **Sequential proton MRS study of brain metabolite changes monitored during a complete pathological cycle of demyelination and remyelination in a lysophosphatidyl choline (LPC)-induced experimental demyelinating lesion model.** *NMR Biomed* 2002;15:293–300